# Data Completeness Estimation for 3-D C-arm Scans with Rotated Detector to enlarge the lateral Field-of-View

Daniel Stromer[1,2], Patrick Kugler[2], Sebastian Bauer[2], Günter Lauritsch[2], Andreas Maier[1]

[1]Pattern Recognition Lab, FAU Erlangen-Nuremberg
[2]Siemens Healthcare GmbH, Forchheim, Germany
daniel.stromer@gmx.de

**Abstract.** In this paper, we describe a method to enlarge the field-of-view of those scan modes by rotating the detector such that instead of the detector width the diagonal of the detector limits the lateral field-of-view for a Short and two Large Volume Scan trajectories. After implementation of the modifications we obtain a gain of 25.8 % in field-of-view diameter accompanied by a simultaneous loss of height of about 50 %. The coverage is increased by 20 % for the Short Scan and by 16.7 % for the Large Volume Scans. After introducing a detector shift trade-off we still increase the coverage field-of-view width while compensating the axial loss. Also a reduced source-to-detector distance has been investigated, which further increases the coverage. Finally, a Helical Large Volume Scan trajectory was simulated leading to the same width gain and coverage but increasing the height by 20.8 % for the maximal shift and 33.3 % for the trade-off version in comparison to a standard Large Volume Scan.

*Disclaimer: The concepts and information presented in this paper are based on research and are not commercially available.*

## 1 Introduction

Current Robotic C-arm X-ray systems using cone-beam imaging allow to calibrate a much wider range of trajectories [1]. Today, there are two clinically used approaches to perform 3-D scans with a multi-axis C-arm system using a circular scan trajectory, the Short Scan [2] and the Large Volume Scan (LVS) [3]. Within the Short Scan, a turn of 180 ° plus fan angle is made to gain the minimal complete dataset for the given geometry. A LVS performs a 360 ° rotation with a detector shift of half a detector length in lateral detector direction. Hereby, the field-of-view (FoV) is nearly doubled. There are situations in the clinical workflow where this extended FoV is still too small to image the whole volume-of-interest. A typical scenario is liver imaging of obese patients. Thus, there is a need to extend the lateral FoV somehow for those kinds of applications.

In the following, a method is shown to enlarge the lateral FoV diameter for Short and LVSs by rotating the detector in such a way that not the detector width but the diagonal of the detector limits the lateral FoV.

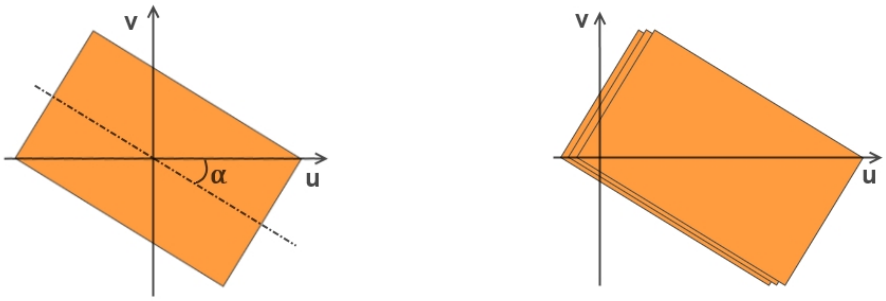


(a) No shift (b) Shifted detector

**Fig. 1.** Rotation of detector by angle $\alpha$ with and without detector shifting.

## 2 Materials and Methods

The methods presented were evaluated using CONRAD [4], a software framework for cone beam imaging in radiology. First, circular trajectories were defined for both scan approaches. The source-to-object distance was set to 600 mm and the source-to-detector distance (SID) to 1200 mm to get the initial FoV. As detector a 620 mm × 480 mm flat-detector was chosen. Acquisitions were made in landscape mode. The origin of the detector's coordinate system is right in the center of the detector with the $u$-axis pointing along the lateral side and the $v$-axis along the axial side of the detector. $v_{max}$ and $u_{max}$ are the axial and lateral measurements of the detector. For the enlargement of the field-of-view, the detector has to be rotated such that the diagonal of the detector lies on the $u$-axis. In the following, we call these scans *Diamond Scans*. Fig. 1(a) shows the detector after turning it by a rotation angle $\alpha$ calculated by:

$$\alpha = \arctan \frac{v_{max}}{u_{max}} \tag{1}$$

### 2.1 Short Scan

For the Short Scan, a C-arm rotation of 200 ° without detector shift is performed for getting a minimal complete dataset for cone beam geometry. A circular trajectory was defined having 200 projection matrices resulting in an average angular increment of 1.0 °. Turning the detector by angle $\alpha$ we get a diagonal of 784 mm. Compared to the previous lateral FoV spread of 620 mm we expect an increase of the coverage by about 26.5 %. With the source-to-object distance being half of the SID, the newly generated coverage should be 392 mm instead of 310 mm.

### 2.2 Large Volume Scan

The Large Volume Scan covers a whole turn of 360 °. The circular trajectory has 180 projection matrices, resulting in an average angulation increment of 2.0 °.

This kind of scan implies a shift of the detector in $u$-direction for half of the detector width enlarging the coverage by a factor of two compared to the Short Scan. Using the given dimensions of the detector, the shift is set to 310 mm. For the Diamond LVS the maximal shift of the detector is given by:

$$s_{max} = \frac{1}{2} \cdot \sqrt{u_{max}^2 + v_{max}^2} \tag{2}$$

For the used trajectory, $s_{max}$ is 392 mm. To ensure a complete data coverage, we set the shift $s$ to 390 mm. The closer the detector is shifted to this limitation, the more loss of information in the area around the $v$-axis is implicated. Fig. 1(b) shows various shifts of the detector in $u$-direction. In case of the maximal shift we increase the lateral FoV to 620 mm or 780 mm for the Diamond Scan, respectively. This corresponds to a lateral FoV diameter gain of about 25.8 %.

### 2.3 LVS with a helical trajectory

A drawback of applying the detector rotation is that axial information gets lost. To compensate this we finally simulate a Diamond Helical LVS. We set five full rotations and selected a pitch as small as possible and as large as necessary. Tests revealed that with the given detector configuration, a pitch of 9 mm is optimal. We assume that by using this setup, the lateral field should stay the same while we extend the axial field with each rotation more and more.

### 2.4 Measurement of Data Completeness

To calculate voxel-wise data completeness for the mentioned scans, a method for arbitrary discretely sampled trajectories was used [5]. The method computes the 3-D coverage of Radon plane normals on a unit sphere and ranges between 0 and 1 at each voxel. To speed up the calculations the image size was set to $64 \times 64 \times 64$ voxels (spacing 16 mm $\times$ 16 mm $\times$ 4 mm). A coverage cut-off value of 0.9 is set.

## 3 Results

### 3.1 Short Scan

For the Short Scan the resulting coverage image of the central slice is shown in the top row of Fig. 2. Fig. 2(a) shows a standard Short Scan whereas Fig. 2(b) shows the Diamond Scan's coverage. By measuring the Diamond Scan's lateral coverage spread an increase of 64 mm was observed which matches our expectations. We achieve a total coverage of 320 mm for the normal Short Scan and 384 mm for the Diamond Short Scan raising the lateral coverage by 20.0 %. Reconstructing the coverage volumes leads to the detector's FoV. Fig. 2(c) shows the forward projection of the standard Short Scan's and Fig. 2(d) of the Diamond Short Scan's coverages. The maximal lateral spread is increased by 160 mm or by a factor of about 25.8 % matching exactly with our expectations. However, it can be seen that the FoV is no more rectangular but diamond shaped.

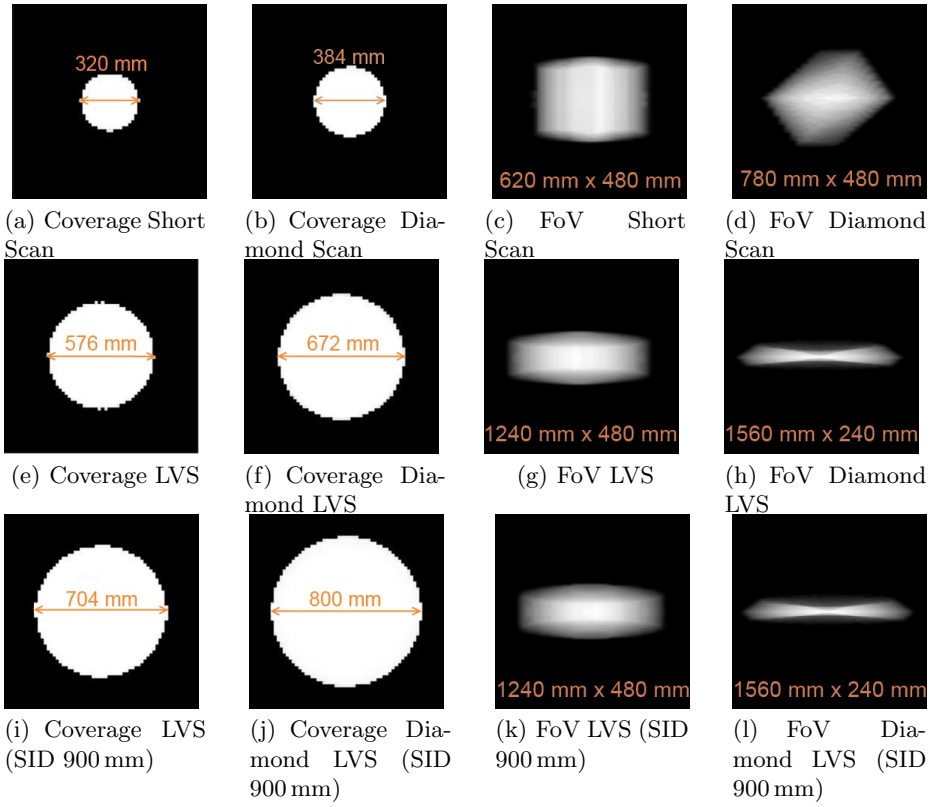


(a) Coverage Short Scan (b) Coverage Diamond Scan (c) FoV Short Scan (d) FoV Diamond Scan

(e) Coverage LVS (f) Coverage Diamond LVS (g) FoV LVS (h) FoV Diamond LVS

(i) Coverage LVS (SID 900 mm) (j) Coverage Diamond LVS (SID 900 mm) (k) FoV LVS (SID 900 mm) (l) FoV Diamond LVS (SID 900 mm)

**Fig. 2.** Central slices of Radon sphere coverages ($c > 0.9$) and detector's FoV for the investigated scan modes. The top row shows the Short Scan, the middle row the LVS and the bottom row the LVS with a reduced SID of 900 mm.

### 3.2 Large Volume Scan

Fig. 2(e) shows the standard LVS coverage whereas Fig. 2(f) shows the Diamond LVS Scan's coverage. We extend the coverage by 16.7 % from 576 mm to 672 mm in total. After reprojecting the coverage volumes, we receive the images shown in Fig. 2(g) for the standard LVS's FoV and Fig. 2(h) for the Diamond Scan's FoV. The lateral width of the FoV is 1240 mm for the standard LVS whereas the Diamond LVS reaches 1560 mm implying an increase of 25.8 % and 320 mm which again matches our expectations. On closer examination it can also be seen that the axial spread is unfavorable as it is rather small and not covered uniformly. It has been halved from 480 mm to 240 mm. To achieve a larger coverage we reduced the SID to 900 mm, simultaneously leading to a decreased spatial resolution. Comparing the coverage from the Diamond LVS (Fig. 2(j)) to the standard LVS (Fig. 2(i)) leads to the result that we improve the lateral coverage by 13.6 % from 704 mm to 800 mm. The FoV's are shown in Fig. 2(k) and Fig. 2(l). The lateral spread of the normal LVS is 1240 mm while for the one with the rotated


(a) Detector shift 390 mm (b) Detector shift 370 mm

**Fig. 3.** Central slices of Diamond Helical LVS ($c > 0.9$) reconstructions with various detector shifts. The frames mark the measured FoV area.

detector 1560 mm could be measured, such that we still achieve the lateral gain of 320 mm in total or 25.8 %, respectively. The newly generated axial FoV spread is still 240 mm what means that we have to deal with a loss of 50 %. Furthermore, we investigated a trade-off between axial loss and lateral gain by reducing the detector shift from the maximal shift to 370 mm. The result is a coverage of 768 mm and a FoV of 1480 mm × 280 mm, which is an axial plus of 40 mm.

### 3.3 LVS with a helical trajectory

Finally, we applied a helical trajectory. Fig. 3(a) shows the obtained FoV. The coverages and the lateral spread of the FoV remain the same but the axial spread of the FoV was extended by about 240 % to 580 mm in comparison to the circular Diamond LVS. We also simulated the trade-off shown in Fig. 3(b). Compared to the helical scan with the maximal shift, we again reduced the lateral FoV by 80 mm but obtain a axial extension up to 640 mm. This is 228 % more than with a circular scan, or 33.33 % more than a standard LVS.

## 4 Discussion

We presented a method for improving the coverage of common 3-D scans by rotating an imaging system's detector such that the diagonal lies on the $u$-axis of the detector coordinate system. Tab. 1 shows the results of the performed simulations compared to each other. With a SID of 1200 mm we increased the lateral FoV by 25.8 % for the presented scan modes but lost 50 % axial information. By reducing the SID to 900 mm we further increased the lateral coverage by another 128 mm and 13.6 %. Finally reducing the detector shift by 20 mm again, led to a decreased axial loss of only 41.7 % instead of 50 % while still achieving a coverage plus of 9.1 % and a lateral FoV plus of 19.4 %. To enlarge the axial FoV, we applied a helical trajectory extending the axial spread. With the maximal possible shift we extend the axial FoV to 580 mm. This is about 20.8 % more than a LVS without detector rotation attains. Applying a detector shift trade-off of −20 mm, an axial spread of 640 mm can be obtained, what means a plus of 33.3 % compared to the standard LVS. We get an interesting shaped

| Scan Mode | SID $[mm]$ | Coverage $[mm]$ | FoV $[mm \times$ mm$]$ |
|---|---|---|---|
| Short Scan | 1200 | 320 | $620 \times 480$ |
| Diamond Short Scan | 1200 | 384 | $780 \times 480$ |
| LVS | 1200 | 576 | $1240 \times 480$ |
| Diamond LVS | 1200 | 672 | $1560 \times 240$ |
| LVS | 900 | 704 | $1240 \times 480$ |
| Diamond LVS | 900 | 800 | $1560 \times 240$ |
| Trade-Off Diamond LVS | 900 | 768 | $1480 \times 240$ |
| Diamond Helix LVS | 900 | 800 | $1560 \times 580$ |
| Trade-Off Diamond Helix LVS | 900 | 768 | $1480 \times 640$ |

**Table 1.** Results of the presented methods compared to each other. Coverage $[mm]$ is the coverage in the isocenter at 600 mm and FoV the resulting FoV from the forward projection of the coverage.

FoV which is able to cover areas with larger lateral spread than the standard LVS which might be suitable for liver imaging. It has to be mentioned that the helical scanning geometry produces a lot of redundantly scanned areas. Using axial collimation could reduce this effect. In this case, we would end at a scanning geometry that is very similar to a diagnostic CT scanner with a long, but very narrow detector.

Thus, we believe, that applying a detector rotation within the mentioned scan modes could be more accurate for recording especially long, slender volumes than present scan methods.

## References

1. Herbst M, Schebesch F, Berger M, Choi JH, Fahrig R, Hornegger J, et al. Dynamic detector offsets for field of view extension in C-arm computed tomography with application to weight-bearing imaging. Medical Physics. 2015; p. 2718–2729.
2. Parker DL. Optimal short scan convolution reconstruction for fan beam CT. Medical Physics. 1982;9:254–257.
3. Strobel N, Meissner O, Boese J, Brunner T, Heigl B, Hoheisel M, et al. Multislice CT. Springer Berlin Heidelberg; 2009.
4. Maier A, Hofmann HG, Berger M, Fischer P, Schwemmer C, Wu H, et al. CONRAD - A software framework for cone-beam imaging in radiology. Medical Physics. 2013;40(11).
5. Maier A, Kugler P, Lauritsch G, Hornegger J. Discrete Estimation of Data Completeness for 3D Scan Trajectories with Detector Offset. In: Handels H, Deserno TM, Meinzer HP, Tolxdorff T, editors. Bildverarbeitung für die Medizin 2015. Berlin, Heidelberg; 2015. p. 47–52.